

Supplementary information

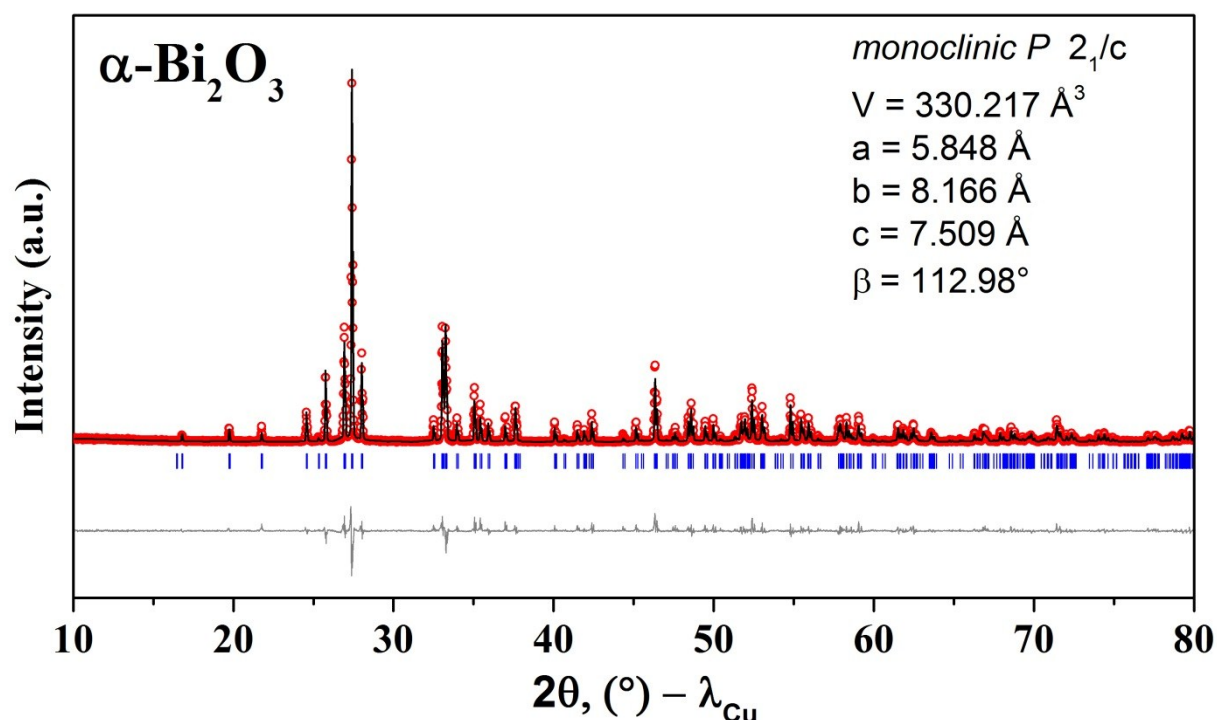


Figure S1: XRD pattern of α - Bi_2O_3 and the corresponding Rietveld refinement. The red circles, black continuous line and bottom grey line represent the observed, calculated, and difference patterns respectively. Vertical blue tick bars are the Bragg positions

Table S1: Structural parameters for $\text{Bi}_4\text{B}_2\text{O}_9$ deduced from the Rietveld refinement of the XRD pattern at room temperature. Isotropic B's were imposed equal for a same chemical species.

Space Group $P 2_1/c$					
$a = 11.1153(8) \text{ \AA}, b = 6.6324(1) \text{ \AA}, c = 11.0447(3) \text{ \AA}, \beta = 91.0465(3)^\circ$					
$V = 814.099(4) \text{ \AA}^3, Z = 4, \text{ density} = 8.17 \text{ g/cm}^3, \text{ Bragg R-factor } 4.48\%$					
Atom	Wyckoff site	x	y	z	B (\AA^2)
Bi1	4e	0.9922(6)	0.4822(4)	0.3467(4)	0.073(2)
Bi2	4e	0.8073(1)	0.0483(5)	0.4921(3)	0.073(2)
Bi3	4e	0.5012(1)	0.4230(6)	0.1595(5)	0.073(2)
Bi4	4e	0.3409(1)	0.4365(5)	0.4818(1)	0.073(2)

O1	4e	0.500(3)	0.107(6)	0.105(1)	1.126(4)
O2	4e	0.383(3)	0.080(3)	0.494(4)	1.126(4)
O3	4e	0.865(2)	0.159(7)	0.282(8)	1.126(4)
O4	4e	0.923(1)	0.157(7)	0.013(4)	1.126(4)
O5	4e	0.187(9)	0.203(1)	0.142(7)	1.126(4)
O6	4e	0.676(2)	0.226(8)	0.367(6)	1.126(4)
O7	4e	0.147(2)	0.242(1)	0.352(7)	1.126(4)
O8	4e	0.343(3)	0.314(4)	0.279(2)	1.126(4)
O9	4e	0.715(2)	0.319(5)	0.154(9)	1.126(4)
B1	4e	0.753(4)	0.235(6)	0.263(3)	1.1439(6)
B2	4e	0.224(4)	0.252(1)	0.253(3)	1.1439(6)

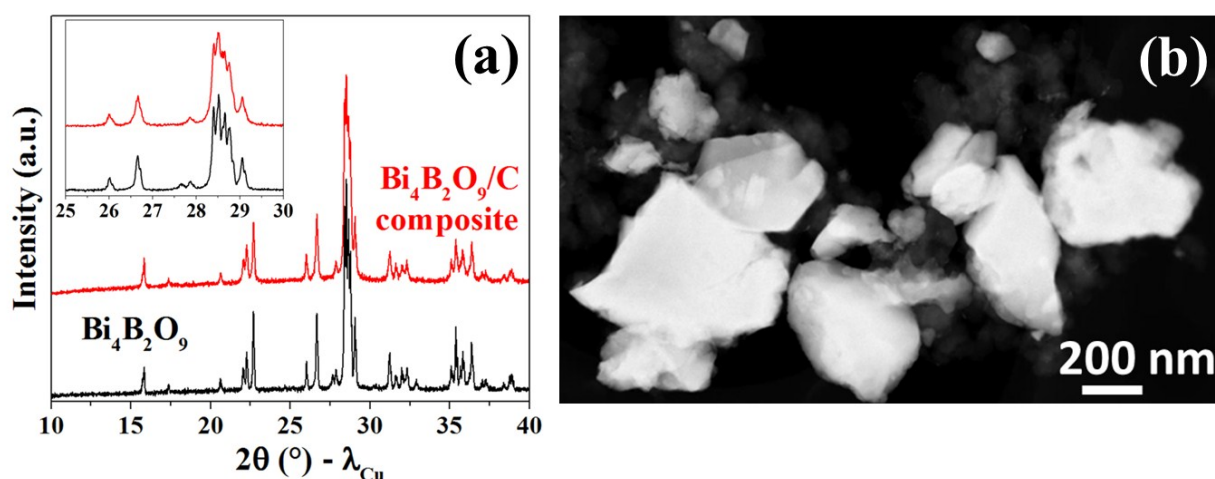


Figure S2: (a) XRD profile of $\text{Bi}_4\text{B}_2\text{O}_9/\text{C}$ composite compared to that of the as synthesized $\text{Bi}_4\text{B}_2\text{O}_9$ indicating the broadening of the reflections as a result of ball milling (inset) Note that the intensity of the $\text{Bi}_4\text{B}_2\text{O}_9/\text{C}$ XRD pattern has been normalized for better comparison. The full width at half maximum (FWHM) value is 0.0145° and 0.0849° for the reflection located at 26.21° 2θ . (b) Representative TEM image for the $\text{Bi}_4\text{B}_2\text{O}_9/\text{C}$ composite.

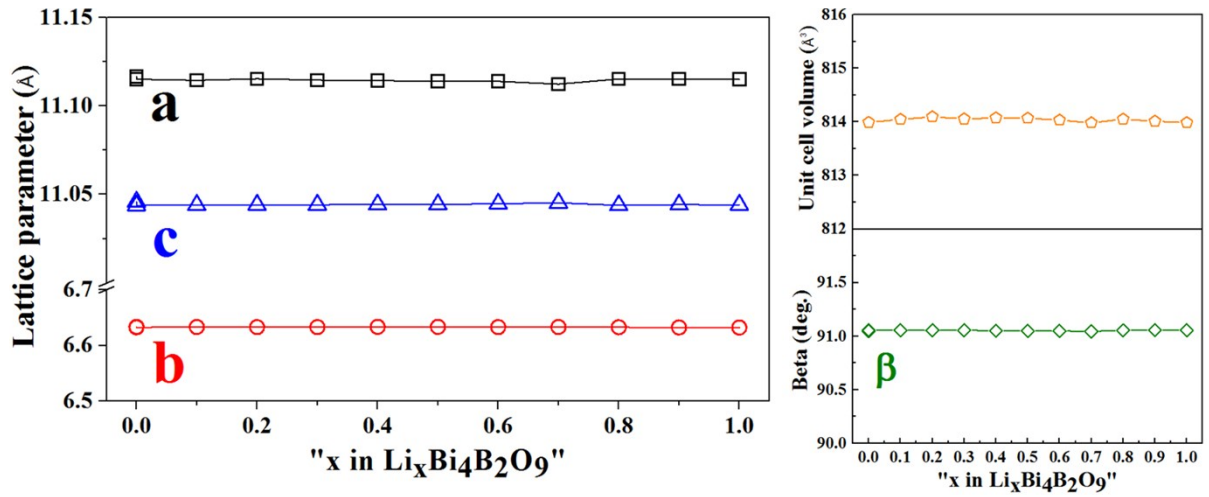


Figure S3: Refined lattice parameter of $\text{Bi}_4\text{B}_2\text{O}_9$ from the *in situ* XRD patterns recording during the initial discharge for a Li uptake of $x = 1$ in " $\text{Li}_x\text{Bi}_4\text{B}_2\text{O}_9$ ".

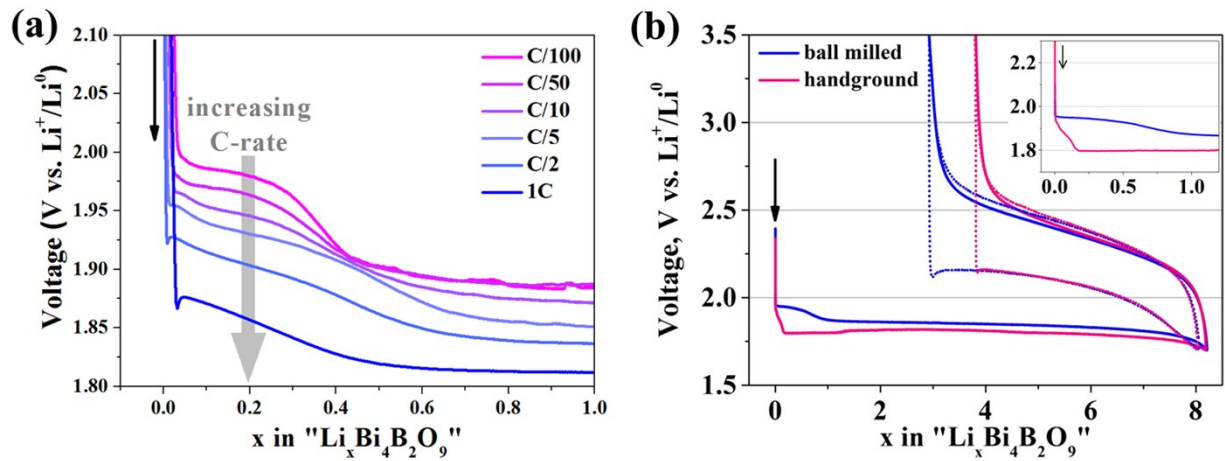


Figure S4: (a) Initial discharge of the $\text{Bi}_4\text{B}_2\text{O}_9/\text{C}$ composite applying different C-rates and (b) comparison of the voltage-composition curve between the ball-milled and hand ground $\text{Bi}_4\text{B}_2\text{O}_9/\text{C}$ composite.

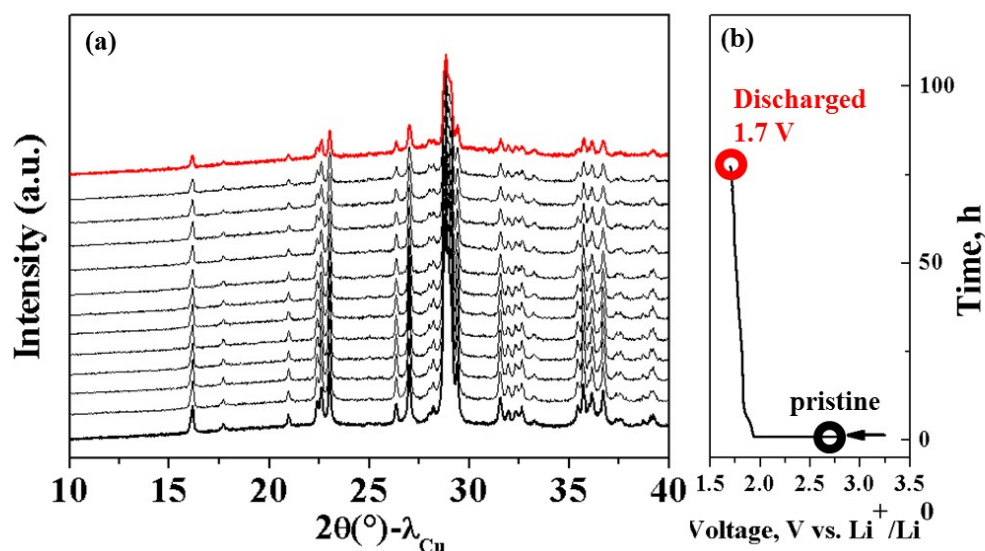


Figure S5: (a) *In situ* XRD pattern recorded for $\text{Bi}_4\text{B}_2\text{O}_9$ discharged to 1.7 at a C/10 rate and (b) the corresponding electrochemical trace.

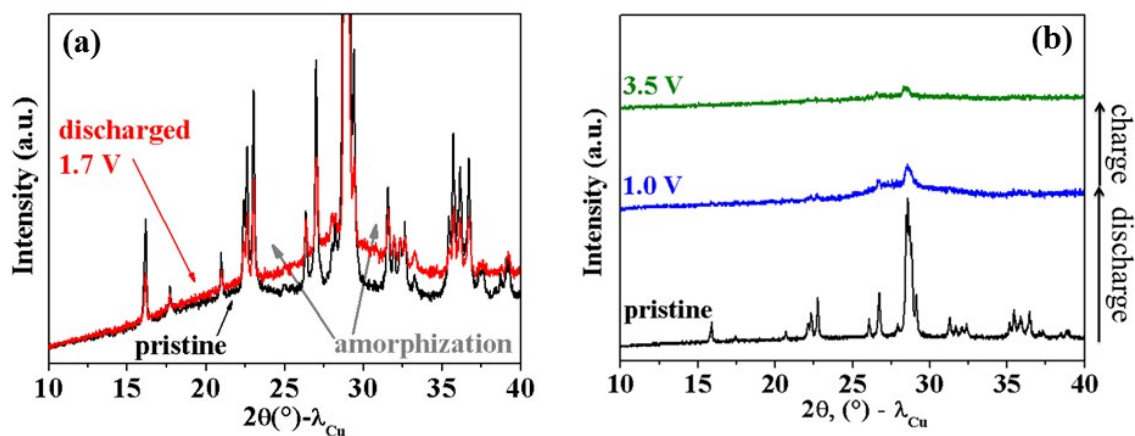


Figure S6: (a) Comparison of the *in situ* XRD pattern of the pristine $\text{Bi}_4\text{B}_2\text{O}_9$ and the discharged state (1.7 V) highlighting the appearance of the bumpy background which is not obvious from Figure S1a. (b) *Ex situ* XRD pattern recorded for $\text{Bi}_4\text{B}_2\text{O}_9$ discharge to 1.0 and subsequent charged to 3.5 V with a C/10 rate.

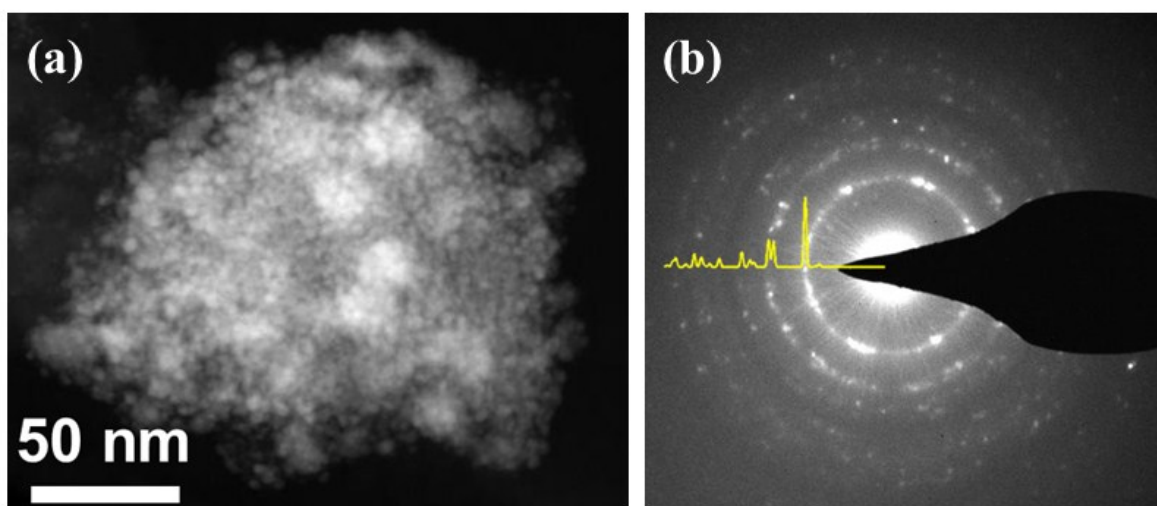


Figure S7: (a) Representative TEM image of a $\text{Bi}_4\text{B}_2\text{O}_9/\text{C}$ sample discharged to 1.0 V and recharged to 3.5 V, and (b) SAED collected from the same sample indicating the presence of elemental bismuth.

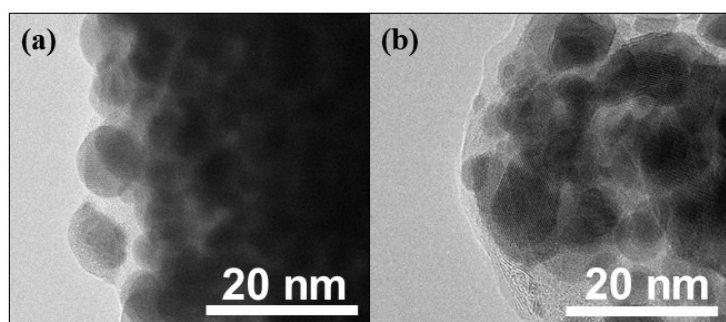


Figure S8: (a) Typical TEM images of the active material discharged at (a) 1.7 V and (b) 1.0 V.

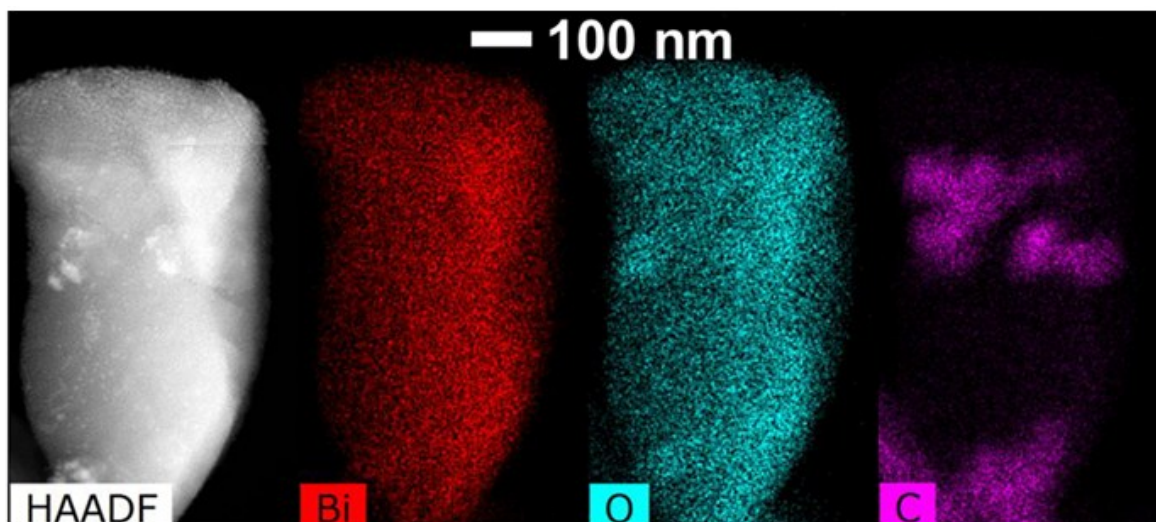


Figure S9: TEM image and the corresponding EDX maps for a $\text{Bi}_4\text{B}_2\text{O}_9$ sample discharged to 1.7 V. Bi, O and C elemental distribution are shown in red, cyan and purple respectively.

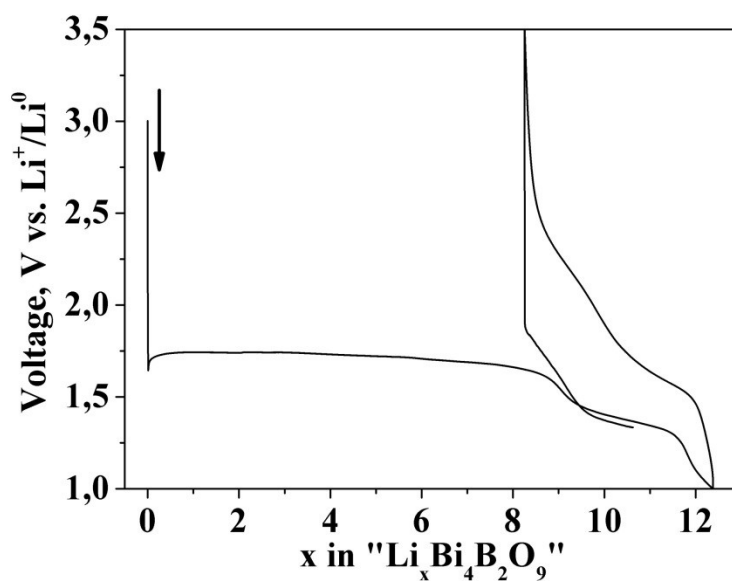


Figure S10: Voltage-composition curve of as synthesized $\text{Bi}_4\text{B}_2\text{O}_9$ versus Li cycled at a C/10 rate between 1.7 and 3.5 V without any conductive additive.